

TECHNIQUES FOR MODELING THERMAL AND MECHANICAL STRESSES GENERATED IN CATALYTIC CRACKER AND COKE DRUM HOT BOXES

Chris Alexander
Stress Engineering Services, Inc.
Houston, Texas USA
chris.alexander@stress.com

Richard Boswell, P.E.
Stress Engineering Services, Inc.
Houston, Texas USA
richard.boswell@stress.com

ABSTRACT

Consideration of heat transfer loading between surfaces during transient and steady state conditions is required when analyzing vessels that involve secondary stresses and low cycle fatigue. Some of the higher stresses occur in enclosed, non-insulated air space regions, referred to as a hot box, between a supporting skirt (or shell) and a vessel. Hot boxes are critical parts of vessel designs in catalytic crackers and delayed coke drums. In coke drum cycles, the sudden heating of the vessel generates significant bending stresses in the skirt, and radiation heat transfer causes a greater area of skirt to be heated when compared to conduction alone. This heat must be removed during the cooling transient or the hot expanded skirt will be pulled by the contracting vessel, resulting in large bending stresses. It is the experiences of the authors that failures to calculate the transient temperatures in the components often underestimate fatigue stresses.

Some of the important elements associated with modeling thermal stresses in hot boxes include using appropriate boundary conditions, radiation and convection conditions, pressure end loads, and conductivities for the insulation materials. This paper emphasizes the importance of performing detailed sensitivity analyses when unknown thermal or mechanical loading conditions exist. Examples include the effects of convection properties within the hotbox and conditions associated with transient loads. Discussions are also provided on the potential geometric issues associated with the use of axisymmetric finite element models. Additionally, this paper discusses the importance of making field measurements to enhance modeling assumptions. Discussions will be provided on the best methods for acquiring field data and the techniques employed.

INTRODUCTION

Hot boxes play important roles in many high temperature pressure vessel systems such as catalytic crackers and coke drums located in refineries by reducing thermal differences between attachments during rapid transients. The materials associated with the hot box region are subjected to non-uniform elevated temperature distributions leading to elevated thermal stresses. Because of the challenges associated with these loading conditions, it is often difficult to design vessels so that stresses are within proper design limits. Some of the important elements associated with modeling thermal stresses in hot boxes include using appropriate boundary conditions, radiation and convection conditions, pressure end loads, and conductivities for the insulation materials.

This paper addresses four primary subject areas:

- Present details on analysis methods used to assess the behavior of a hot box located in a cat cracker. This presentation discusses modeling techniques used to incorporate a range of potential loading conditions (referred to as *bounding*).
- Appendix 4 of Division 2 of the ASME Boiler & Pressure Vessel Code provides specific guidance for selecting appropriate design stresses limit. In spite of the fact that Division 2 has been in use for over 35 years, there is still confusion among many designers about how to properly distinguish between design and operating stresses when presenting results. Discussions are provided on how to use the Appendix 4 *Hopper Diagram* in selecting appropriate design stress limits.
- Discuss some of the potential pitfalls when modeling radiation and specifically differences that exist when comparing results for two and three dimensional models. Comparisons are also made for results calculated by both ABAQUS and ANSYS, the two primary finite element codes employed by pressure vessel engineers.
- Discussions on the best methods for collecting field data and the importance that field data has on validating analytical models. It is the authors' observations that many engineering firms perform analyses of complex pressure vessel systems subjected to thermal loads without any effort to capture actual field data, which often produce incorrect modeling assumptions.

The following sections provide details on the four subjects presented above.

HOT BOX ANALYSIS OF A CAT CRACKER

The catalytic cracking unit, known as the cat cracker, is one of the most important units in a refinery. The cat cracker takes the heavier, less valuable molecules from the distillation process and breaks them down into smaller ones. These smaller, more useful and therefore more valuable molecules are used for manufacturing petrol and provide feedstocks for other applications such as those found in chemical plants.

The following sections provide details on the modeling techniques that were used to calculate stresses in the hot box region of the cat cracker. The presentation involves discussions on modeling techniques, loads generated by heat transfer and mechanical loads, and details on the calculated stresses compared to design stresses.

Modeling Techniques

A location designated as a *hot box* is developed by the three shell intersection located in a cat cracker. This region of the cat cracker was modeled with the geometry provided in **Figure 1**. The finite element model employed an axisymmetric formulation using two-dimensional continuum elements (all loads are axisymmetric in nature). As noted in this figure, the analysis considered two conditions for the hot box: one where the hot box was filled with insulation material and a second condition where the hot box was empty. In actuality, even when the original design does not consider the presence of insulation material in the hotbox, it is prone to collect debris that acts like insulation material.

Figure 2 provides details on the loading and boundary conditions used in modeling the cat cracker. Also included in this figure is a close-up view of the finite element mesh in the vicinity of the hot box that includes elements for the insulation material (these elements could be turned ON or OFF during analyses as required). **Figure 3** is a schematic diagram that has been color-coded to indicate the location of materials in the cat cracker design. Material properties were assigned to each region of the finite element model. In the heat transfer analysis, material conductivities were used in computing the nodal temperature distribution. In the structural analyses, the coefficients of thermal expansion were used to compute thermal stresses and the temperature-dependant elastic moduli contributed to the calculated stresses.

Heat Transfer Model

The heat transfer analysis was used to compute temperature profiles within the finite element model considering maximum operating temperatures. From an analytical standpoint, the finite element method permits the computation of temperature at each node within the model. The following variables contribute to the calculated temperatures.

- Temperature-dependent thermal conductivities for steels and insulating materials.
- Maximum operating temperatures in the disengager/stripper and regenerator regions were used.
- Using the value provided in the design specification, a film coefficient of 60.5 BTU/hr-ft²·°F (340.7 W/m²·°C) was used for all internal surfaces other than the hot box region. The position of the catalyst bed within the model was not considered in terms of generating a static head.
- An external temperature of 32 °F was assumed as a worst case condition with an external convection film coefficient of 1.362 BTU/hr-ft²·°F. As a check, nodal temperatures were calculated assuming an external bulk temperature of 120 °F with minimal effect on the elevated internal temperatures
- The thermal model in the hot box incorporated both convection and radiation. A bulk temperature of 700°F was assumed for both of these heat transfer mechanisms. A convection film coefficient of 2.045 BTU/hr-ft²·°F (11.63 W/m²·°C) and a radiation emissivity of 0.8 were used.

The heat transfer model assumed steady state conditions with no considerations for transient time-dependant behavior. The calculated nodal temperatures were used as input into the structural model for computing thermal stresses.

Structural Model

While the heat transfer model computed nodal temperatures due to operating conditions, the structural models were used to compute

actual stresses due to both design and operating loads. These stresses are compared to the allowable limits of stress intensity per ASME Section VIII, Division 2 (and Division 1 for elevated temperatures).

Using the methods of Appendix 4 of Division 2, design loads include internal pressure and weight, while the operating loads include internal pressure, weight and thermal loads. For additional clarification, **Figure 4** is included that shows the *hopper diagram* of Fig. 4-130.1 from Appendix 4 of Division 2. This figure shows the difference in how design loads (solid lines) and operating loads (dashed lines) are integrated into the stress analyses.

The structural models incorporated the internal pressures by applying pressures to the appropriate interior surfaces of the model. End loads that incorporated pressure and weight were applied at the appropriate cut surfaces (refer to **Figure 2** for details on the respective application regions).

Selected Hot Box Thermal Loading Conditions

The thermal conditions in the hotbox contribute significantly to the stress distribution in the three-shell intersection of the cat cracker. For this reason, a range of thermal conditions that might exist in the hot box region were considered. This exercise involved bounding the problem with the intent being to assist the designer in developing a greater understanding about the behavior of this region of the cat cracker. Four possible conditions were considered in the hot box.

- **Designer-specified design:** Combination of convection and radiation in the hot box was specified. A bulk temperature of 700°F was assumed for both of these heat transfer mechanisms. For convection a film coefficient of 2.045 BTU/hr-ft²·°F (11.63 W/m²·°C). For radiation an emissivity of 0.8 was used.
- **Insulated Condition:** Insulation was modeled inside the hot box region (elements inserted into this region). The insulating material was assumed to be mineral wool with a nominal thermal conductivity of approximately 0.8 BTU-in /hr-ft²·°F.
- **Convection-only:** An upper bound model was calculated using only convection with an elevated bulk temperature of 1373 °F and a convection film coefficient of 2.045 BTU/hr-ft²·°F.
- **Catalyst filled:** This model considered that the hot box was filled with catalyst material. The catalyst was assumed to have a thermal conductivity of 12.0 BTU-in /hr-ft²·°F. This is basically the same model as the Insulated Condition discussed above, except the elements inside the hot box have conductivities for catalyst material rather than insulation materials.

For each of the above conditions, a heat transfer model was analyzed and a complete structural model was then processed to include weight, internal pressure, and thermal loading. One of the primary purposes of this paper is to present results for these assumed operating conditions and the impact of the results on the final design.

Analysis Results

There is a large body of data that can be presented based on the analysis results for the cat cracker; however, the intent in this presentation is to address the impact that specific hot box conditions have on the calculated stresses. For this reason, a minimum amount of data is presented.

Figure 5 provides an overall view of the model and the calculated temperature distribution. Convective heat transfer was modeled on the exterior surface of the vessel and a bulk temperature of 32 °F was assumed. A minimum metal temperature of approximately 340°F was

computed. **Figure 6** shows a close-up view of the three-shell intersection. Note the absence of the insulation material in the hot box region that was used included in some of the analyses.

Figure 7 and **Figure 8** are stress intensity contour plots for the operating case with the insulation and refractory materials removed for clarity. For additional clarity, these figures show regions of high stress with contour bands plotted in **RED** that exceed 12,200 psi. In contrast to the results obtained for the design loads, the stresses due to operating loads are significantly higher. This is due to the presence of thermal loads and stresses generated by thermal expansion associated with the temperature distribution in the model.

To permit comparison of the calculated stresses to Code design stresses, eleven zones representing thirteen sections for stress linearization were selected. These sections are referred to as *stress classification lines* (SCLs). Across these sections, linearized stresses are computed that represent the same net bending moment as the actual stress distribution. This method of stress classification is required when making comparison to the Code allowable stresses. **Figure 9** shows the selected zones, including details on SCL 3 and SCL 4 in the connection between the 304H, 310H, and F22 materials in the vicinity of the hot box. The stresses in the other SCLs were relatively low and not of interest to the design problem.

Referring to the listing presented previously for the four assumed hot box thermal conditions (i.e. designer-specified conditions, insulated condition, convection only, and catalyst filled), results are presented. For each of these models, a heat transfer model was analyzed and a complete structural model was processed that included loading due to weight, internal pressure, and thermal loading. **Table 1** provides a summary of the results for each of these cases for stress classification lines 3A, 3B, 4A, and 4B. This is the region where the SA-240-310H transition piece is located. Also included in this table are the FEA-calculated temperatures from the heat transfer model and the appropriate $2.0 S_m$ limits. As noted in reviewing the data in **Table 1**, the only thermal combination that produced stresses that exceeded the designer-specified design limit is the convection-only model at location 3B. Although these conditions are conservative and may not be realistic or typical for normal operating conditions, they represent an upper bound condition that results in generating stresses that exceed the specified design limits.

Closing Comments

Results have been presented for an analysis that was performed to address stresses in the hot box region of a cat cracker. One objective of this presentation was to show the effects of how assumed thermal conditions can impact stresses generated considering mechanical and thermal loads. The methods presented can be employed by design engineers when questions exist about possible loading conditions. Through bounding efforts, the analyses results can be used confidently by assuring the appropriate levels of conservatism are used in developing a particular pressure vessel design.

SELECTING PROPER DESIGN STRESS LIMITS

Thermal stresses are always combined with operating stresses per Appendix 4 of Division 2 of the ASME Boiler & Pressure Vessel Code. In spite of the fact that Division 2 has been in use for over 35 years, confusion still exists among many designers about how to properly distinguish between design and operating stresses when presenting results. Of particular importance from a design standpoint

are the allowable stresses permitted by the Code. For example, Division 2 of the Code limits Primary plus Secondary Membrane plus Bending Stresses ($PL + Pb + Q$) to $3.0S_m$; however, some designers limit this stress class to $2.0 S_m$. Although for many structural design applications using $2.0 S_m$ may be over-conservative (compared to the conventional stress intensity limit of $3.0 S_m$), it is warranted in situations where excessive deformations can occur. For the cat cracker, excessive deformation can lead to cracks in the refractory lining that could lead to non-uniform temperature profiles resulting in locally-elevated stresses.

Refer once again to the Hopper Diagram presented in **Figure 4**. Remembering that this figure shows the difference in how design loads (solid lines) and operating loads (dashed lines), the following observations are made in relation to selecting design stress limits for analyses involving stresses due to thermal and mechanical loads.

- Design loads include internal pressure and weight (solid lines drawn in **Figure 4**)
- Operating loads include internal pressure, weight, and thermal loads (dashed lines drawn in **Figure 4**)
- Stress intensities are used when making comparison between the calculated and the (current) Code allowable stresses. Future editions of the code will be based on Von Mises stresses.
- Stress linearization is required to separate the calculated stresses into the appropriate stress categories
- Stress gradients through the vessel wall due to internal pressure are not primary bending (P_b), but are classified as secondary bending, Q .
- Code Case 1489-2 validates extending the stress tables for Division 2 at elevated temperatures using the stress tables for Division 1.

MODELING RADIATION IN PRESSURE VESSELS

Many pressure vessels in refining processes involve high temperature for molecular cracking, and are operated in cyclic service. In some cases the cycles are for batches of material processed, and in other cases the cycle duration is years. For many vessels, the operating temperatures cause significant weakness in the steel components and thus require careful design for economy and safety. An issue that must often be included is *low cycle fatigue* when a vessel is expected to cycle from ambient to extreme temperatures less than 10,000 times. *Low cycle fatigue* is often the result of constrained thermal stresses. *High cycle fatigue* applies to vibration type loadings where a significant number of low amplitude stresses are accumulated.

Two basic modes of heat transfer between steel components include conduction and convection. Conduction includes heat flow through the material, and is a function of the thermal resistance and the thermal capacitance of the specific metals. It is a function of time and distance. Convection includes heat loss and gain from the metal to the vapor surrounding it such as air. This is a function of boundary layer turbulence as well as the environment temperature. Often these are combined into an equivalent value to facilitate calculation of the heat transfer at the surface boundary when insulation is involved. Both of these methods are a consequence of atomic and molecular excitation energy.

A third mode, and a subject addressed in this paper, is *radiation heat transfer*. Radiation heat transfer provides a fast track for heating attachments to pressure vessels undergoing rapid heat-up transients.

Thermal radiation is electromagnetic radiation emitted from a body as a result of its elevated temperature relative to its environment [3]. It is propagated at the speed of light and is a function of the frequency and wavelength of the radiation. It operates in a spectrum higher than visible light and its propagation takes place in the form of discrete quanta called quantum representing a particle of energy. Using mass and momentum calculations of particles, it is shown that energy density of the radiation is proportional to the fourth power of the absolute temperature. Because energy is transferred from a hot body to a colder body, the amount of energy can be described as a function of the temperatures ($T_1^4 - T_2^4$). The significance is this becomes a very important heat transfer component when one part of a vessel is heated and cooled much faster than another adjacent and facing part. This is often found at skirt junctions supporting process vessels.

Heat flows as a function of area, and the area for radiation heat transfer is described by shape factors to relate how much of a body surface is seen by another body surface. The distance separating two specific bodies is part of the geometric view and the density of heat flow when the fixed surfaces (plates) are parallel to each other. In most instances the surfaces are at angles to each other and these real surfaces do not perfectly diffuse and radiation is not emitted uniformly in all directions. Interestingly, non-conductors emit more energy normal to the surface, and electrically conductive materials emit more energy at large angles to the surface.

Lastly in this background discussion is the surface condition. A blackbody will absorb all of the energy presented to it. Non-black bodies will reflect a portion of the energy like a mirror and hence not absorb all of the energy available. Energy can be reflected back and forth several times between surfaces. *Irradiation* describes the total incident radiation density and *radiosity* describes the density leaving, both reflected and emitted. Thus, we see that calculation of radiant energy heat transfer is possible but not trivial, and is actually difficult to accurately perform.

Heat Transfer Analysis Using Modern FEA Codes

Modern finite element programs provide features to calculate radiation heat transfer, and as in all similar results, final temperature distributions must be checked for accuracy. There are two common forms of structural heat transfer model discussed in this paper: axis-symmetric and 3-D solid with planes of symmetry. Without having abundant experience with temperature measurements on vessels, the authors would not have recognized that at least two major codes did not accurately calculate radiation heat transfer for 3-D solid models.

To evaluate the performance of several finite elements codes and address issues related to modeling techniques, analyses were performed using ABAQUS and ANSYS. These analyses addressed the ability of each of these codes to model radiation and specifically the performance of two-dimensional axisymmetric models compared to three-dimensional solid models.

Figure 10 and **Figure 11** provide the calculated temperature profiles for the fill and quench cycles of the cat cracker, respectively. As noted in these plots, comparison of data involves analyses of three-dimensional ANSYS and ABAQUS models, as well as two-dimensional ABAQUS models.

The following observations are made when comparing the data plotted in **Figure 10** and **Figure 11**.

- There is a 20 to 23 degree difference in temperature prediction between the ANSYS and ABAQUS three-dimensional models
- There is a significant difference in the calculated temperatures between the three and two dimensional models. The maximum difference during fill is about 150° F and during the quench it is approximately 60° F
- These results indicate that cavity radiation formulations may not be the same for two and three dimensional finite element models.

During the heating transient, more heat is provided to the skirt in the hot box zone by radiation, then by conduction alone. During cool down phases of the transient this *extra* heat capacity must be removed primarily via conduction, since the skirt and vessel are more closely matched in temperature. This in turn creates additional bending stress at the attachment weld between the skirt and vessel (e.g. coke drum). A typical total stress range is composed of 40 percent from heat up and 60 percent from cool down.

Development of the Hot Box Design

One of the earlier technical papers to discuss the benefits of “hot box” design was published by two Kellogg engineers in New York [2]. This was a Kellogg patented feature. This paper used rigorous hand calculations for thermal gradients, forces and moments, and resulting stress to compare insulated joint versus open boxes for efficiency in transferring heat and temperature from the vessel shell to the supporting skirt. Different weld designs were also discussed, particularly for delayed coker vessels. The conclusions were that likelihood of cracking of the attachment weld would be less using “hot box” details. In this paper, the design is referred to simply as an “improved skirt support” with an “air gap retained in the crotch formed by the skirt and vessel”. However, the authors of this paper [2] only mention radiation and convection heat transfer in their discussion, and do not suggest they have calculated, but rather rely on simplifications of the thermal gradients.

MAKING FIELD MEASUREMENTS

Temperature measurements on operating vessels should consider several issues to improve accuracy. First is the selection of thermocouple style. The authors have found the welded separated junction style to be the only type to accurately measure large transients. This method uses low power capacitive discharge welding to attach each wire. The base metal between the wires becomes a common dissimilar junction to both leads, and the measurement represents the average temperature of the surface between them. Other sheath type styles will always have thermal resistance and capacitance creating a time delay and desensitization. In refinery applications the authors generally use K-Type wires.

Second, the locations of the measurements are important especially for the skirt junctions. For recreating the transient in a finite element model the vessel temperature immediately above the attachment weld is important. To validate the thermal models a vertical distribution on the skirt can be used to describe the region of the hot box (top, middle, bottom, and below) and to describe the heat sink of the foundation on the bottom of the skirt. Measurement on the shell inside the hot box are difficult to install, but often the vessel knuckle and cone beneath the hot box can have location through the commonly found insulation.

Third, the data recording plan must provide accurate measurement at appropriate intervals. Data rates faster than a scan per minute are not often necessary. Structural transients may change as fast as 100 °F per

minute when the energy is available, but the data detail acquired at intervals less than one minute is generally not useful.

Cables should be secure and protected, and not allowed to form any contacts other than at the desired measurement point. A thermocouple measurement will always be at the junction of the wire pair closest to the measuring instrument. Several common problems occur when the cable is in contact with hot metal such as a nozzle flange, melting the insulation and forming a junction at another location. This has happened when the cable was routed when the vessel was cold, and the nozzle became hot during operation. Connectors will form junctions if allowed to get wet or soak in water puddles. Lastly, a temperature measurement equal to the average of the hot location and ambient will be seen when one of the two wires is in contact with the vessel or ground in any point along the cable. This has occurred when a cable is severely scraped, or when a strand of metallic over-braid has punctured the insulation on the wire or in contact at a terminal screw.

Several figures are included that provide details on how field measurements should be made, especially with regards to selecting the appropriate locations for installing thermocouples. **Figure 12** is a field diagram that shows the designated locations where thermocouples were installed. The reader will also note that the locations for installing two high temperature strain gages (HTSGs) are also marked on this figure. One of the important points in studying this figure is the spacing of the thermocouples relative to the location where the elevated temperature gradients were expected. **Figure 13** provides the data that was collected from the ten positioned thermocouples. It is clear from the plotted data that the results confirm that the thermocouples were properly positioned to permit an accurate mapping of the temperature field.

CONCLUSIONS

This paper has provided discussions on the modeling, analysis, and monitoring of hot box designs. The importance of performing detailed sensitivity analyses is addressed if unknown thermal loading conditions exist. Examples include the effects of convection properties within the hotbox, conditions associated with transient loads, and potential geometric issues associated with the use of axisymmetric models. Additionally, this paper discusses the importance of making field measurements to enhance modeling assumptions.

Although not exhaustive, it is clear based on the presented information that accurate modeling of pressure vessels subjected to thermal loads requires that engineers consider a range of loading conditions and consider options associated with bounding problems, especially when unknown thermal conditions are present. Along the same lines, it is important that engineers recognize the importance of making field measurements and take advantage of the available technology when opportunities present themselves.

REFERENCES

- [1] ASME Boiler & Pressure Vessel Code, Section VIII, Division 2, published by the American Society of Mechanical Engineers, New York.
- [2] Weil, N. A., and Murphy, J. J., *Design and Analysis of Pressure-Vessel Support Skirts*, ASME Journal and Engineering for Industry, February 1960.
- [3] Holman, J. P., *Heat Transfer*, Second Edition, McGraw Hill, 1968.

Table 1: Case 3 Results for Various Thermal Hot Box Conditions (including data for the FEA-calculated temperatures, stresses, and 2.0S_m design limit)

SCL	Material	Designer-specified Condition	Insulated Condition	Convection Only	Catalyst Filled
3A	SA-240-310H (25 Cr - 20Ni)	971°F 11.8 ksi 32.4 ksi (2.0S _m)	1097°F 19.8 ksi 29.8 ksi (2.0S _m)	1229°F 19.3 ksi 25.3 ksi (2.0S _m)	1084°F 20.5 ksi 30.4 ksi (2.0S _m)
3B	SA-240-304H (18Cr - 8Ni)	971°F 19.3 ksi 30.5 ksi (2.0S _m)	1097°F 24.9 ksi 27.6 ksi (2.0S _m)	1229°F 25.6 ksi 23.4 ksi (2.0S_m)	1084°F 25.0 ksi 27.6 ksi (2.0S _m)
4A	SA-336 F22 Class 3 (2-1/4Cr - 1Mo)	837°F 34.2 ksi 43.7 ksi (2.0S _m)	1019°F 19.8 ksi 31.7 ksi (2.0S _m)	1226°F 24.0 ksi 26.2 ksi (2.0S _m)	1000°F 16.8 ksi 32.8 ksi (2.0S _m)
4B	SA-240-310H (25 Cr - 20Ni)	837°F 19.2 ksi 32.7 ksi (2.0S _m)	1019°F 18.9 ksi 31.4 ksi (2.0S _m)	1226°F 21.3 ksi 23.4 ksi (2.0S _m)	1000°F 16.2 ksi 32.1 ksi (2.0S _m)

Notes:

- (1) The 2.0 S_m value is the average of hot (FEA-calculated temperature) and cold allowable stresses. For conservatism, this stress limit was selected over the conventional stress limit of 3.0S_m as provided in Appendix 4 of the Code.
- (2) All material data taken from Section II, Part D of the Code.
- (3) Data for each cell includes the FEA-calculated temperature, FEA-calculated stress intensity, and the 2.0S_m design limit.
- (4) Data in BOLD exceeds the specified 2.0S_m design limit.

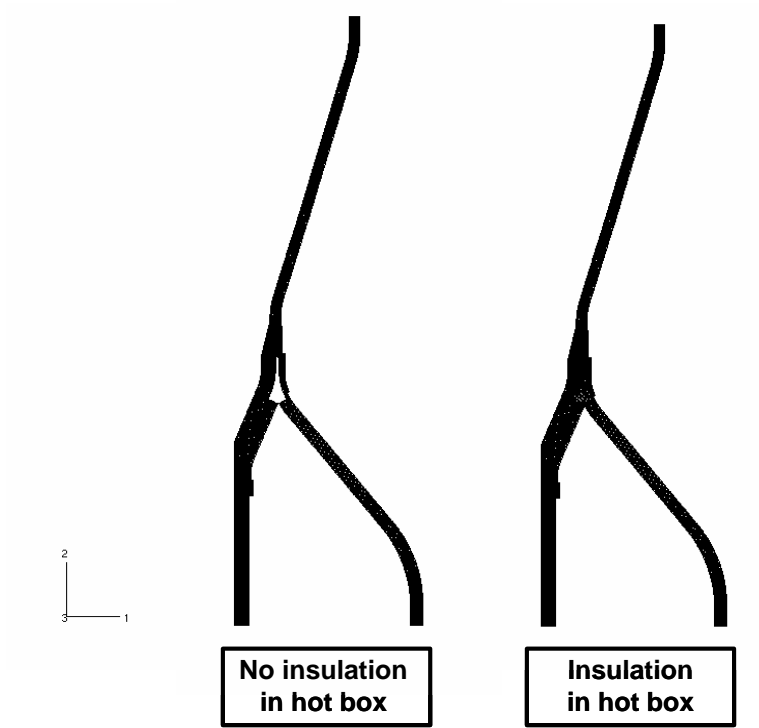


Figure 1: Axisymmetric finite element model used to analyze the hotbox (model considering hot box with and without insulation)

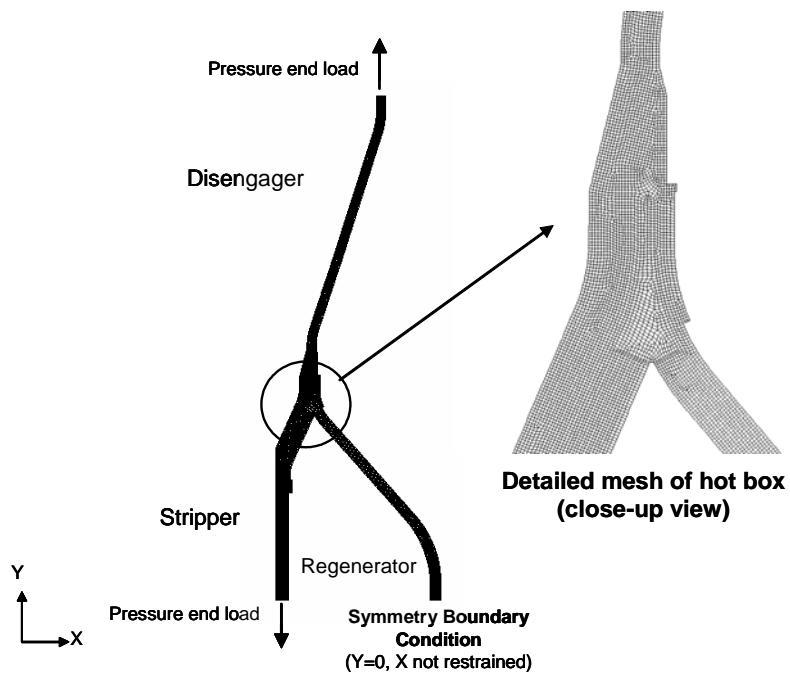


Figure 2: Details on boundary conditions and the mesh near the hot box

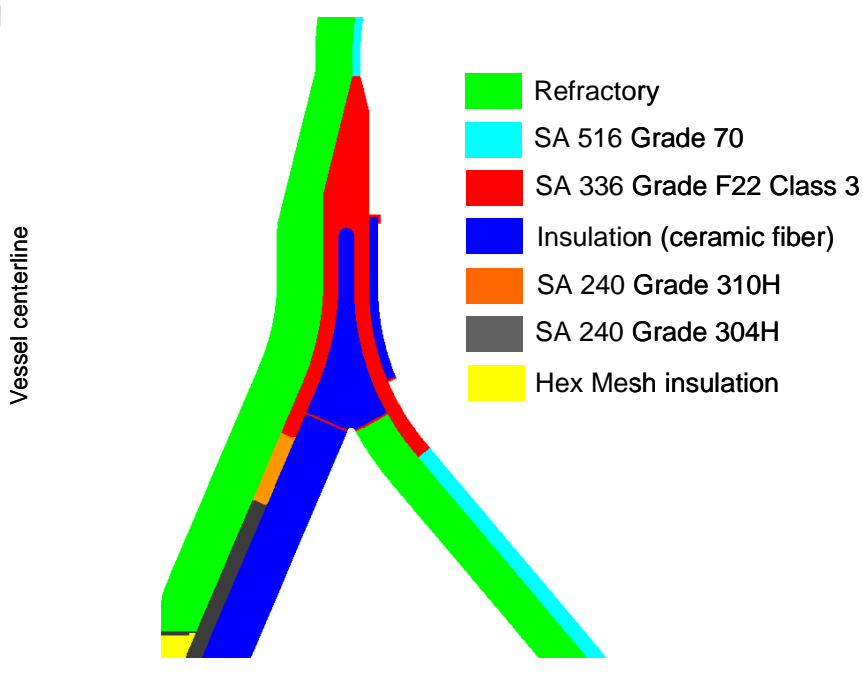


Figure 3: Materials used in finite element model

APPENDIX 4 — MANDATORY

Fig. 4-130.1

Stress Category	Primary			Secondary Membrane plus Bending	Peak
	General Membrane	Local Membrane	Bending		
Description (For examples, see Table 4-120.1)	Average primary stress across any solid section. Excludes discontinuities and concentrations. Produced only by mechanical loads.	Average stress across any solid section. Considers discontinuities but not concentrations. Produced only by mechanical loads.	Component of primary stress proportional to distance from centroid of solid section. Excludes discontinuities and concentrations. Produced only by mechanical loads.	Self-equilibrating stress necessary to satisfy continuity of structure. Occurs at structural discontinuities. Can be caused by mechanical load or by differential thermal expansion. Excludes local stress concentrations.	(1) Increment added to primary or secondary stress by a concentration (notch). (2) Certain thermal stresses which may cause fatigue but not distortion of vessel shape.
Symbol [Note (3)]	P_m	P_L	P_b	Q	F

Combination of stress components and allowable limits of stress intensities.

——— Use design loads
 - - - Use operating loads

Figure 4: Stress categories and limits of stress intensity (Fig. 4-130.1. from Code)



Figure 5: Temperature distribution in cat cracker (units of °F)

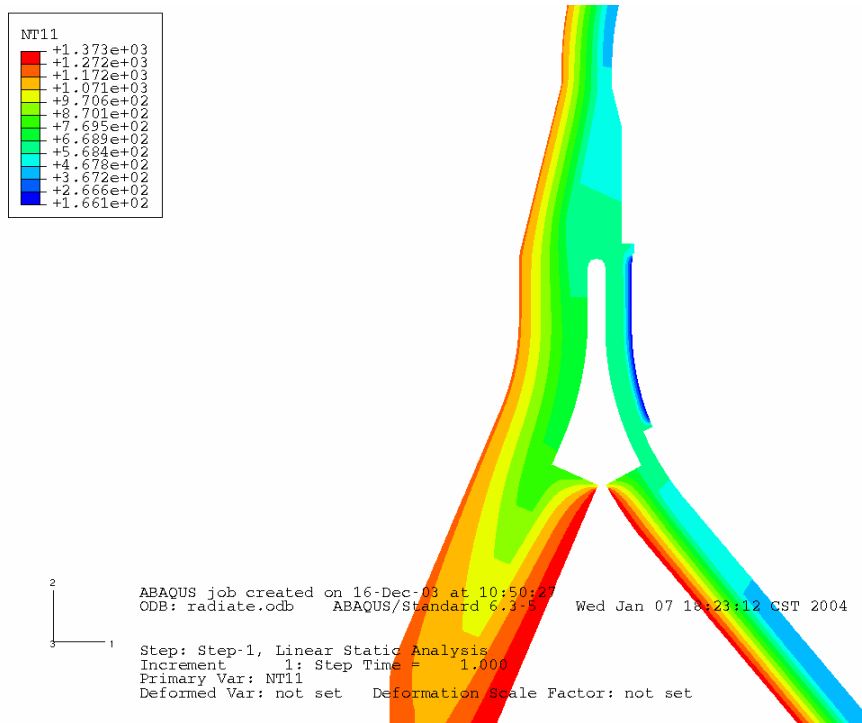


Figure 6: Temperature distribution in shell intersection region (units of °F)

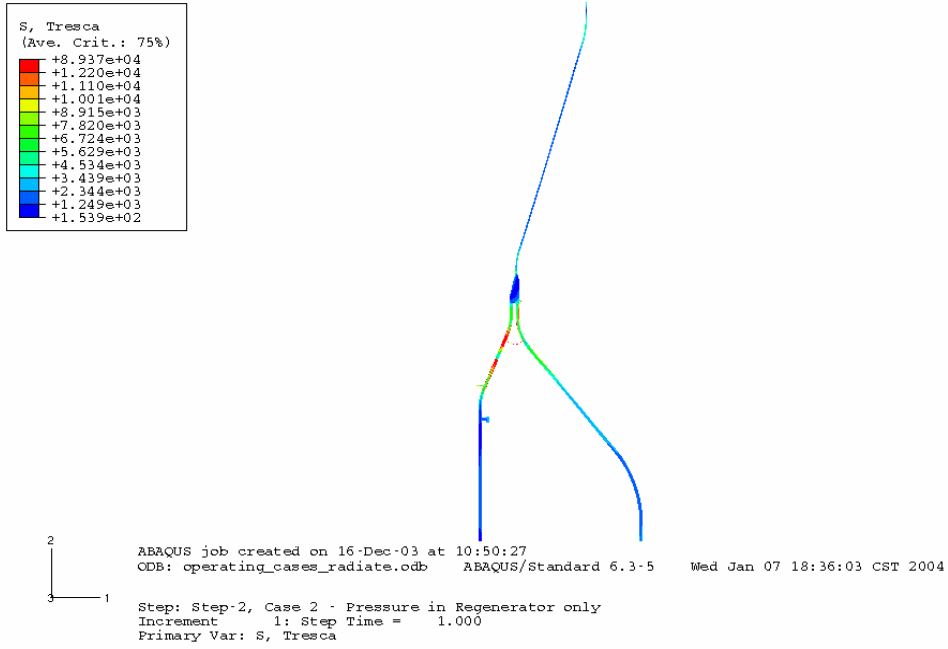


Figure 7: Stress contour plot for Operating Case
 (no pressure in disengager/stripper, pressure in regenerator, thermal loads)

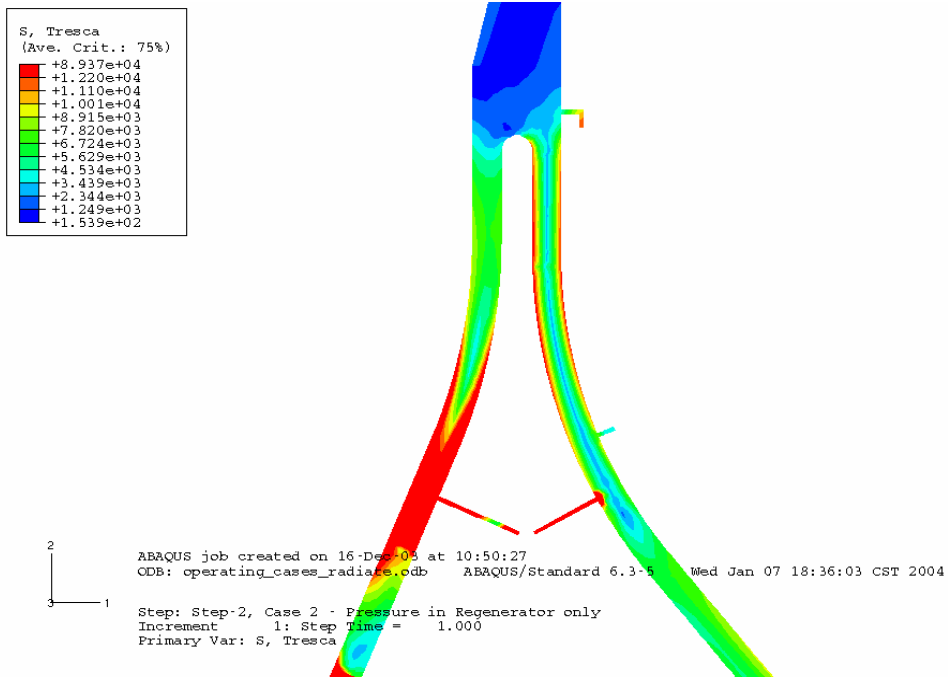


Figure 8: Close-up view of stress contour plot for Operating Case
 (no pressure in disengager/stripper, pressure in regenerator, thermal loads)

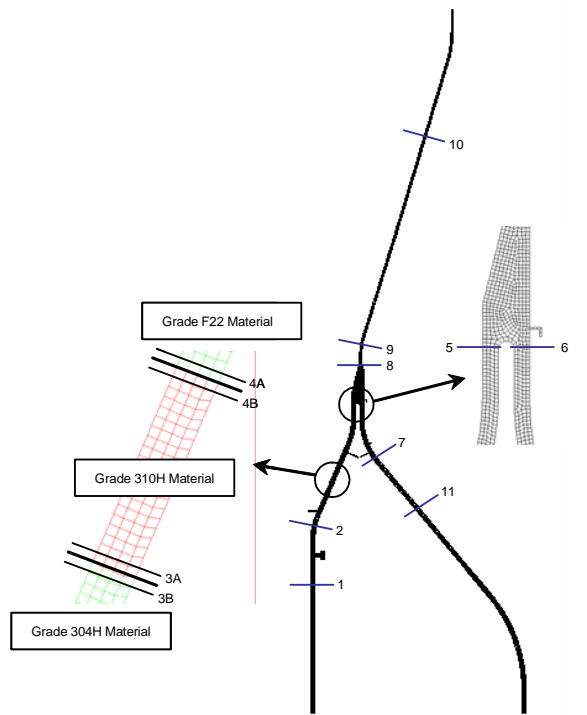


Figure 9: Location of stress classification lines

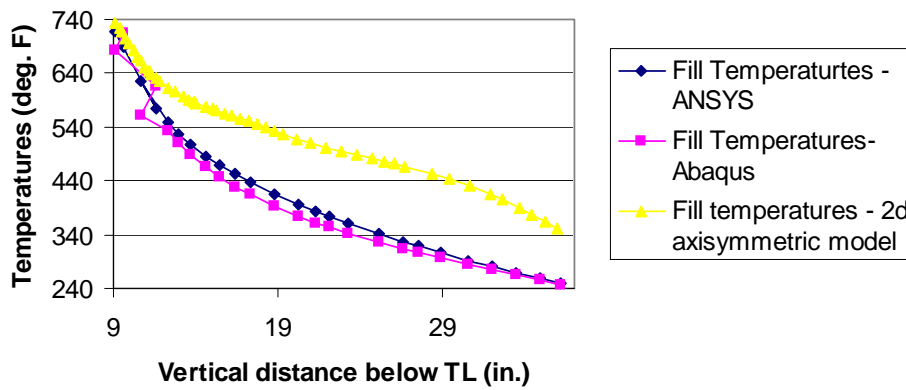


Figure 10: Comparison of calculated temperatures during the FILL cycle

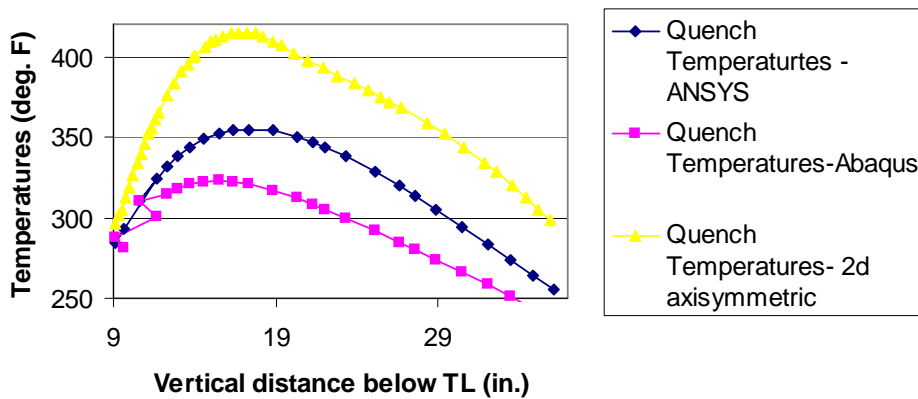


Figure 11: Comparison of calculated temperatures during the QUENCH cycle

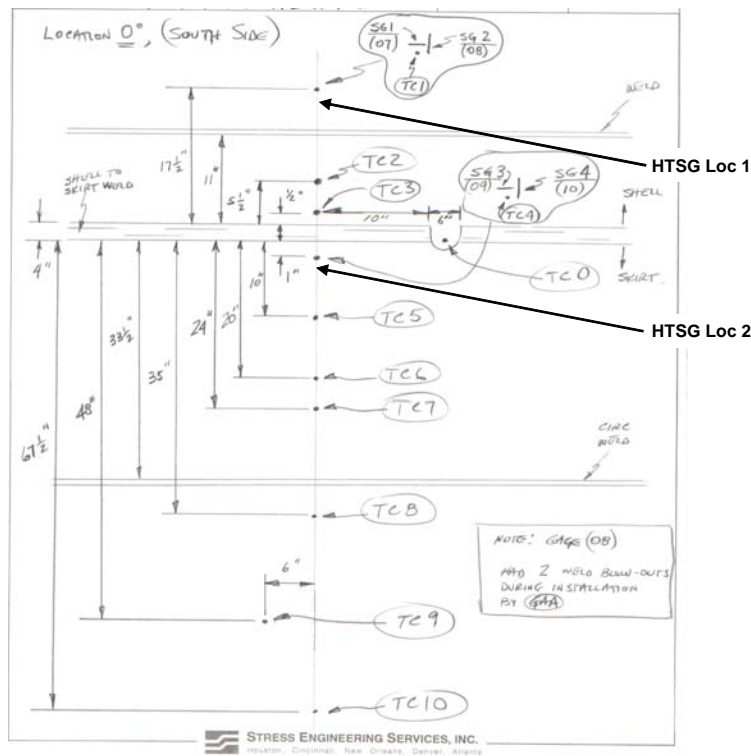


Figure 12: Measured temperatures during the QUENCH cycle

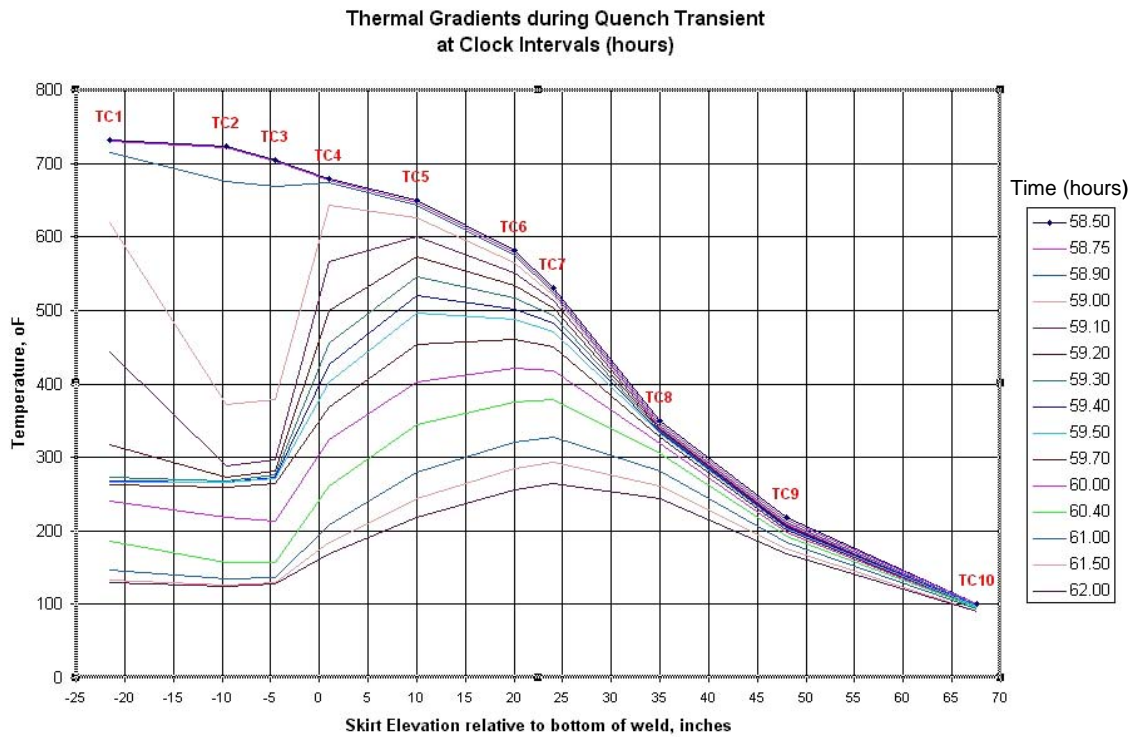


Figure 13: Measured temperatures during the QUENCH cycle